A&A 462, L1–L4 (2007)
DOI: 10.1051/0004-6361:20066590

Astronomy & Astrophysics

Letter to the Editor

The possibility of detecting Sagittarius A* at 8.6 μm from sensitive imaging of the Galactic center

R. Schödel[1], A. Eckart[1,2], K. Mužić[1], L. Meyer[1], T. Viehmann[1], and G. C. Bower[3]

[1] I. Physikalisches Institut, Universität zu Köln, Zülpicher Str. 1, 50937 Köln, Germany
e-mail: [rainer;eckart;muzic;meyer]@ph1.uni-koeln.de
[2] Max-Planck-Institut für Radioastronomie, Auf dem Hügel 69, 53121 Bonn, Germany
[3] Astronomy Department and Radio Astronomy Laboratory, University of California, Berkeley, CA 94720, USA

Received 18 October 2006 / Accepted 16 November 2006

ABSTRACT

Context. Sagittarius A* (Sgr A*) at the center of the Milky Way is a black hole accreting at extremely sub-Eddington rates. Measurements of its emission in the infrared and X-ray domains are difficult due to its faintness and high variability.
Aims. The Galactic center was observed at 8.6 μm in order to detect a mid-infrared (MIR) counterpart to Sgr A*, parallel to NIR observations. The goal was to set constraints on possible emission mechanisms.
Methods. Imaging data were acquired with the adaptive-optics assisted NIR instrument NACO and the MIR instrument VISIR at the ESO VLT.
Results. We present MIR imaging data of an unprecedented quality in terms of spatial resolution and sensitivity. An extended ridge of emission is found to be present in the immediate vicinity of Sgr A* thereby rendering any detection of a point source difficult. No MIR point source related to Sgr A* was detected during the observations. We derive a tight upper limit of 22 ± 14 mJy (dereddened) on any possible point source present during the observations in the night of 4/5 June 2006. The absence of a flare in simultaneous observations at 2.2 μm and the low limits on any possible variability in the MIR strongly suggest that Sgr A* was in a quasi-quiescent state during this night. During the night from 5 to 6 June 2006, Sgr A* was found to be variable on a low level at 3.8 μm. No point source at 8.6 μm was detected during the simultaneous MIR observations. Due to the poorer atmospheric conditions, a higher upper limit of 60 ± 30 mJy was found for Sgr A* at 8.6 μm during the second night.
Conclusions. The observations are consistent with theoretical predictions. If the published models are correct, the observations demonstrate successfully that a 8.6 μm counterpart of Sgr A* can be easily detected in its flaring state. Spectral indices derived from simultaneous observations of flaring emission from Sgr A* at NIR and MIR wavelengths will enable us to distinguish between different kinds of flare models.

Key words. Galaxy: center – Galaxy: nucleus – accretion, accretion disks

1. Introduction

The center of the Milky Way harbors a supermassive black hole of $3.6 \times 10^6\,M_\odot$ (e.g., Schödel et al. 2002; Ghez et al. 2003; Eisenhauer et al. 2005). The non-thermal source related to this supermassive black hole, Sagittarius A* (Sgr A*), radiates at only 10^{-9}–10^{-10} times its Eddington luminosity from radio wavelengths to the X-ray domain. Its low luminosity is consistent with emission from so-called radiatively inefficient accretion flows, a jet, or a combination of the two models (e.g., Yuan et al. 2002, 2003; Bower et al. 2004; Shen et al. 2005).

X-ray and near-infrared (NIR) counterparts to Sgr A* were only discovered with the availability of sensitive, high-resolution instruments for these wavelengths. It was found that Sgr A* is highly variable at these wavelengths, showing flaring emission on time scales of ~60–100 min, with flux increases up to 100 at X-rays and up to 10 in the NIR (e.g., Baganoff et al. 2001; Genzel et al. 2003). The variability at X-ray and IR wavelengths appears to be simultaneous (Eckart et al. 2004, 2006a). At MIR wavelengths, only upper limits to the flux of Sgr A* have been reported so far (Stolovy et al. 1996; Telesco et al. 1996; Cotera et al. 1999; Eckart et al. 2006a). The detection of Sgr A* at MIR wavelengths is difficult due to the lower spatial resolution compared to NIR wavelengths, the general difficulties of imaging in the thermal IR regime, and the presence of warm dust near Sgr A*. Warm dust is associated with the mini-spiral gas streamers that pass close to Sgr A*. Therefore, Sgr A* is no isolated point source in the MIR, and its detection requires high image quality, above all high spatial resolution, in order to achieve a sufficiently high contrast. Here, we report on new MIR observations, using the European Southern Observatory's MIR imager and spectrograph VISIR at the Very Large Telescope (VLT) on Cerro Paranal in Chile.

Although Sgr A* was not detected, the acquired images are – in terms of sensitivity and spatial resolution – the highest-quality 8.6 μm-images of the Galactic center (GC) region published up to now, allowing us to report the so far tightest upper limit on the 8.6 μm flux of Sgr A*. Even more interesting is that we can show – via simultaneously acquired adaptive-optics NIR imaging data – that the infrared flux of Sgr A* agrees well with models of the quiescent/low activity emission. This information allows us to conclude that – according to currently accepted theoretical models – Sgr A* can be easily detected at MIR wavelengths during a bright flare. Such an observation will allow the NIR-to-MIR spectral slope of Sgr A* during flares to be derived and thus allow us to distinguish between different flare models.

Table 1. Summary of observations with VISIR and NACO at the ESO VLT used in this work.

Date	$t_{\rm start}$ [UTC]	$t_{\rm stop}$ [UTC]	$\lambda_{\rm c}$[a] [μm]	$\Delta\lambda$[b] [μm]	DIT[c] [s]	$NDIT$[d]	N[e]	Seeing[f] [$''$]
29 May 2006	04:55	08:01	3.80	0.62	0.2	150	108	0.6$''$
05 June 2006	04:55	08:01	8.59	0.42	0.02	98	1104	0.6$''$
06 June 2006	04:33	07:37	8.59	0.42	0.02	98	1104	1.5$''$
05 June 2006	04:55	08:01	2.18	0.35	30	1	62	0.6$''$
06 June 2006	04:33	07:37	3.80	0.62	0.2	150	1104	1.5$''$

[a] Central wavelength of the filter; [b] FWHM of the filter; [c] detector integration time; [d] number of detector readouts averaged online; [e] total number of images of the target that were acquired; [f] average optical seeing conditions during the observations.

2. Observations and calibration

The GC was observed in the MIR N-band with the ESO VLT unit telescope 3 (UT 3) using the MIR imager/spectrograph VISIR (Lagage et al. 2003, 2004) in the nights of 4/5 and 5/6 June 2006. The pixel scale was 0.075$''$ per pixel. The PAH 1 filter with a central wavelength of 8.59 μm and half-band width of 0.42 μm was used. The standard nodding (~330 deg east of north) and chopping (with a chop throw of 30$''$) technique was used. Standard data reduction was applied, i.e. the sky background acquired during the chopping and nodding observations was subtracted from the images of the target and individual frames were combined with a simple shift-and-add technique. Dithering was applied during the observations, leading to an FOV in the combined mosaic images of ~30$''$ × 30$''$. The seeing during the observations on 5 June 2006 was good enough to result in a PSF FWHM of ~0.3$''$, close to the diffraction limit of the VLT at 8.6 μm.

In this work, we also use NIR-imaging data that were obtained parallel to the MIR data with the adaptive optics imager/spectrograph NACO at the ESO VLT. On June 5, the data were obtained in the *K*s-band in polarimetric mode with a pixel scale of 0.013$''$ per pixel. The data reduction and flux calibration were identical to the procedures described in Eckart et al. (2006b) and in Meyer et al. (2006, A&A, in press). The L'-band (3.8 μm) imaging data were obtained with NACO/VLT on 29 May and 6 June 2006 with a pixel scale of 0.027$''$ per pixel. The reduction of the L'-band data was standard and identical to the data-reduction procedures described in Muzic et al. (2006, A&A, submitted). Details of the NIR and MIR observations are listed in Table 1. The total integration time of the observations corresponds to $DIT \times NDIT \times N$, as given in the table. The total integration time during both MIR observations was thus 36 min.

Flux calibration was achieved by observations of the standard star HD 178345 (14.32 Jy in the PAH 1 filter, see ESO VISIR web site and Cohen et al. 1999). The isolated standard star was also used the PSF reference for image deconvolution.

The astrometric reference frame could be established via the positions and proper motions of the stars IRS 3, IRS 7, IRS 9, IRS 14NE, IRS 12N, IRS 2L, IRS 6E, and IRS 29, which were published by Ott (2004). All of these stars were detected on the VISIR image as point sources. The positions of these eight stars were used to solve transformation equations up to the second order. The accuracy of the astrometric solution could be checked by choosing sub-groups of seven out of the eight stars and repeating the transformation. Also, we compared the measured astrometric position of the stars IRS 16NW, IRS 16C, and IRS 29 to their predicted positions. The position of Sgr A* could thus be established with a 1σ uncertainty of 0.03$''$ (less than half a pixel) in the MIR data. This is about a factor of 10 better than in previous work (Stolovy et al. 1996). There are two main reasons

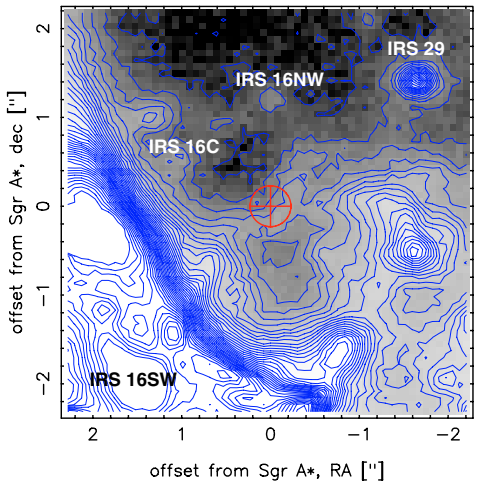

Fig. 1. Sgr A* and its immediate environment at 8.6 μm. Direct shift-and-add image. Contour lines as in are plotted in steps of 0.5 mJy from 0.5 to 20 mJy per pixel (one pixel corresponds to 0.075$''$×0.075$''$). Some well known sources are labeled. The red circle has a radius corresponding to the FWHM of the diffraction limited beam size (~0.25$''$) and is centered on the position of Sgr A*. The astrometric accuracy is ≤0.03$''$.

for this increased astrometric accuracy: on the one hand, the high sensitivity and spatial resolution of the VISIR data and, on the other, the improved IR position of Sgr A* due both to precise positions and proper motions of stars in the NIR (e.g., Genzel et al. 2000; Ott 2004) and to the well-known position of Sgr A* in the IR reference frame via SiO maser sources (e.g., Reid et al. 2003).

Figure 1 presents the flux-calibrated direct shift-and-add image of the central arcseconds around Sgr A* for the night of 4/5 June 2006. Significant signal power was found to be present at the diffraction limit (>60%, estimated by aperture photometry).

3. Flux limits on Sgr A* at 8.6, 3.8, and 2.2 μm

A Lucy-Richardson deconvolved and beam-restored version of the image from Fig. 1 is shown in Fig. 2. The deconvolved and beam-restored image resembles the original image closely, but emphasizes some of the finer details. There is a dust ridge present very close to the position of Sgr A*, where it bends from an east-west extension to a southeast-northwest direction. In earlier MIR observations of the GC, Stolovy et al. (1996) found very similar structures near Sgr A*. Due to their high spatial resolution and sensitivity, the new data show much richer details, however. Even some stars, such as IRS 29, IRS 16NW and IRS 16C (labeled in Fig. 1) can be detected. In spite of the high quality of the data, no obvious point source is present at the position of Sgr A*. We conclude that the source coincident with

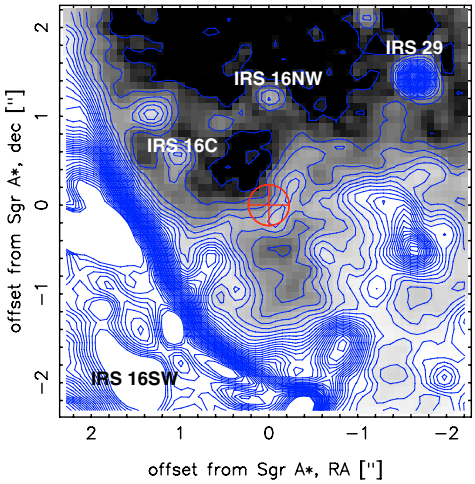

Fig. 2. The Lucy-Richardson deconvolved and beam-restored version of the image shown in Fig. 1, with identical labeling and contour lines. We derive fluxes of 22 ± 5, 21 ± 5, and 180 ± 20 mJy for the point sources IRS 16C, IRS 16NW, and IRS 29 (without extinction correction).

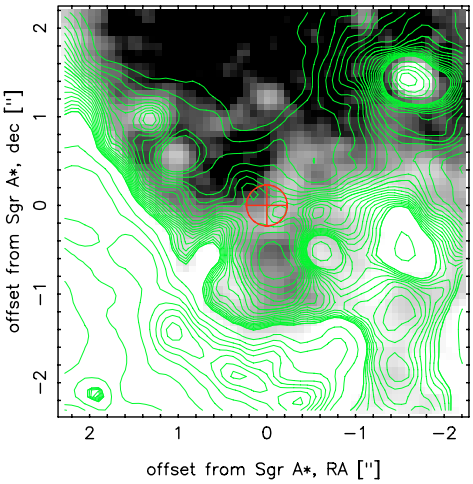

Fig. 3. Contours of diffuse L'-band emission overplotted onto the VISIR 8.6 μm image. Contour levels are drawn between 10 and 200 μJy in steps of 10 μJy and between 0.1 and 2 mJy in steps of 0.1 mJy.

Sgr A* that was reported by Stolovy et al. (1996) was most probably related to the background emission of the dust ridge and not to Sgr A* itself. All the flux appears to originate in the dust ridge. This assumption can be used to obtain a first, simple flux estimate for Sgr A*. Such an estimate can be obtained by adding or subtracting point sources of given flux at the position of Sgr A* and checking whether the shape of the dust ridge is altered perceptibly in the images. After testing various flux levels, we estimate that a point source at the position of Sgr A* that is present in the image cannot be brighter than ∼5 mJy.

With AO L'-band imaging, Eckart et al. (2006a) and Ghez et al. (2005) demonstrate the presence of a dust blob between about 0.03″ and 0.15″ southwest of Sgr A*. As discussed by Eckart et al. (2006a), it is probably this blob that is responsible for most of the MIR emission near the position of Sgr A* when the latter is in a quiescent state. This blob is clearly visible in the MIR images presented here and forms part of the dust ridge. Therefore, a second way of estimating the flux of a putative point source near Sgr A* can be obtained by trying to account for the extended dust emission. For this purpose we used a high-quality L'-band image obtained with NACO in the night 29/30 May 2006. The *StarFinder* (Diolaiti et al. 2000) code was used to extract the stars from the image (including a point source due to the emission from Sgr A*) and thus to obtain an image of the diffuse emission at 3.8 μm. This image was smoothed, transformed, and scaled (with the help of the IDL routines POLYWARP and POLY_2D) to fit the scale, orientation, and resolution of the MIR data. Flux calibration of the L'-band data was achieved by using the published fluxes of the sources IRS 16C and IRS 33N (Blum et al. 1996). Figure 3 shows the diffuse 3.8 μm flux superposed as contour lines onto the MIR image from the right panel of Fig. 1. The median ratio of the diffuse flux at the two wavelengths in a circular area of 0.75″ around Sgr A* is 29 ± 7. This value was used to scale the diffuse flux present in the L'-band data and to subtract it from the MIR image. Here it is important to note that the flux density ratio is much higher in other areas of the mini-spiral. In the northern arm it can be up to 100. Therefore we obtain a conservative estimate of the remnant flux. After subtraction of the scaled diffuse 3.8 μm emission, we find an upper limit on the flux of a putative point source at the position of Sgr A* of 8 ± 5 mJy. Following Lutz et al. (1996), this corresponds to an extinction-corrected flux of 22 ± 14 mJy for the image obtained on 5 June 2006. The lower data quality on 6 June 2006 leads to a higher upper limit of 60 ± 30 mJy (extinction corrected) on any possible Sgr A* counterpart.

During the simultaneous observations at 2.2 μm on June 5, no counterpart to Sgr A* was detected. The upper limit for the flux of Sgr A* was determined to 2 ± 1 mJy. Although the quality of the L'-band observations from June 6 was fairly low (due to bad seeing, poor AO correction and electronic noise on the detector), a weak variable counterpart of Sgr A* could be detected. Its variability was measured to be a factor $\lesssim$2 and its extinction (Lutz et al. 1996) corrected flux to be 10 ± 5 mJy.

4. Discussion

A central question is whether Sgr A* was really in a state of quasi-quiescence when the MIR observations were taken or whether Sgr A* is generally too faint to be detected at MIR wavelengths, even when a flare occurs. We argue that Sgr A* was in a state of quasi-quiescence during the observations on 5 June 2006 for three reasons. (a) The simultaneous observations with NACO at 2.2 μm show that Sgr A* was not detected at 2.2 μm, i.e. ăno NIR flare was observed. (b) Models predict the emission of Sgr A* at 8.6 μm during a flare to be up to 10 times stronger than the upper limit reported by us (see Fig. 4). (c) Differential imaging allows us to derive tight upper limits on the variability of Sgr A* at 8.6 μm during the observations. From a difference image between the data from 5 June and 6 June an upper limit of 15 ± 10 mJy can be derived on any possible variability of Sgr A* between these two days. The high quality data from 5 June allowed an estimate of the upper limit to the variability of Sgr A* during the observations from differential imaging between individual images (∼30 s of integration time, with 1.5 to 2.5 min time between them) taken during this night to 10 ± 6 mJy. Our conclusion is that Sgr A* was indeed in a state of quasi-quiescence during the MIR observations at 8.6 μm.

The lower quality of the June 6 data leads to higher limits of 30 ± 20 mJy for variability between the individual images. The L'-band observations show that Sgr A* was continuously variable during the observations on 6 June. The simultaneously acquired upper limit on the average flux of Sgr A* at 8.6 μm and the limits on shorter timescale variability at this wavelength are consistent with the measurements at 3.8 μm.

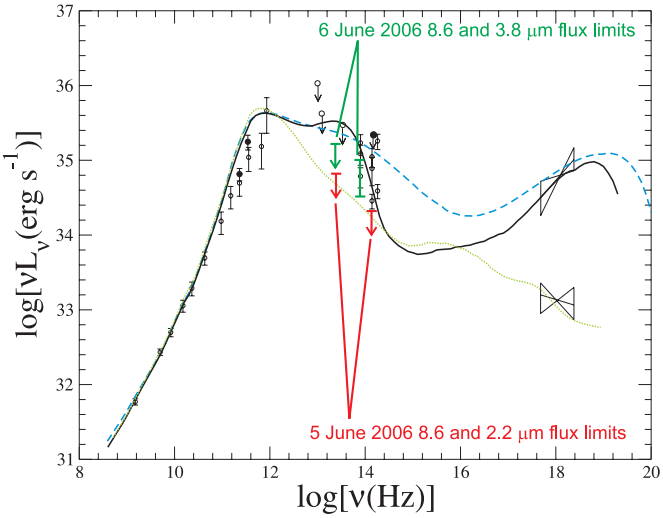

Fig. 4. Emission models for Sgr A* (Yuan et al. 2003, 2004). The upper limit on the flux of Sgr A* at 8.6 μm determined in this work is indicated together with the simultaneously measured (NACO/VLT) flux at 3.8 μm on June 6 and the upper limit on the 2.2 μm emission on June 5 superposed onto RIAF models of the quiescent (dotted line) and flaring (dashed and solid lines) emission from Sgr A*. All flux measurements were corrected for extinction.

Measurements of the Sgr A* quiescent and flaring emission are indicated in Fig. 4 along with theoretical models (data and models taken from Yuan et al. 2003, 2004). The simultaneous measurements at 2.2, 3.8, and 8.6 μm derived in this work are indicated in the figure. Two conclusions can be drawn. (a) The acquired upper limits on the IR flux density of Sgr A* at 2.2 and 8.6 μm set tight constraints on the quasi-quiescent emission and are consistent with the theoretical models shown in the figure. The measurements at 3.8 and 8.6 μm are consistent with the models, too. The measurements also agree with the synchrotron/SSC models presented by Eckart et al. (2006a). Published jet models predict significantly higher fluxes in the MIR (see Falcke & Markoff 2000; Yuan et al. 2002), but can probably be easily adapted to account for the new upper limits. (b) VISIR at the ESO VLT is sensitive enough to detect flaring emission from Sgr A* during a bright flare without difficulty and during a fainter flare during periods of good and stable atmospheric conditions. When combined with simultaneously-acquired NIR measurements, the MIR-to-NIR spectral index will allow a flare model where the X-ray emission is due to acceleration of electrons that produce NIR synchrotron radiation that is up-scattered into the X-ray domain (steep MIR-to-NIR slope) to be distinguished from a model where the NIR emission is due to synchrotron emission from electrons heated to a higher temperature, while the X-ray emission is due to synchrotron emission from some electrons that were accelerated into a hard power law distribution (flat MIR-to-NIR slope).

Acknowledgements. Part of this work was supported by the German *Deutsche Forschungsgemeinschaft DFG* Sonderforschungsbereich project number SFB 494. We thank the referee for her/his helpful comments.

References

Baganoff, F. K., Bautz, M. W., Brandt, W. N., et al. 2001, Nature, 413, 45
Blum, R. D., Sellgren, K., & Depoy, D. L. 1996, ApJ, 470, 864
Bower, G. C., Falcke, H., Herrnstein, R. M., et al. 2004, Science, 304, 704
Cohen, M., Walker, R. G., Carter, B., et al. 1999, AJ, 117, 1864
Cotera, A., Morris, M., Ghez, A. M., et al. 1999, in The Central Parsecs of the Galaxy, ed. H. Falcke, A. Cotera, W. J. Duschl, F. Melia, & M. J. Rieke, ASP Conf. Ser., 186, 240
Diolaiti, E., Bendinelli, O., Bonaccini, D., et al. 2000, A&AS, 147, 335
Eckart, A., Baganoff, F. K., Morris, M., et al. 2004, A&A, 427, 1
Eckart, A., Baganoff, F. K., Schödel, R., et al. 2006a, A&A, 450, 535
Eckart, A., Schödel, R., Meyer, L., et al. 2006b, A&A, 455, 1
Eisenhauer, F., Genzel, R., Alexander, T., et al. 2005, ApJ, 628, 246
Falcke, H., & Markoff, S. 2000, A&A, 362, 113
Genzel, R., Pichon, C., Eckart, A., Gerhard, O. E., & Ott, T. 2000, MNRAS, 317, 348
Genzel, R., Schödel, R., Ott, T., et al. 2003, Nature, 425, 934
Ghez, A. M., Duchêne, G., Matthews, K., et al. 2003, ApJ, 586, L127
Ghez, A. M., Salim, S., Hornstein, S. D., et al. 2005, ApJ, 620, 744
Lagage, P.-O., Pel, J.-W., Claret, A., et al. 2003, in Instrument Design and Performance for Optical/Infrared Ground-based Telescopes, ed. M. Iye, & A. F. M. Moorwood, Proc. SPIE, 4841, 923
Lagage, P. O., Pel, J. W., Authier, M., et al. 2004, The Messenger, 117, 12
Lutz, D., Feuchtgruber, H., Genzel, R., et al. 1996, A&A, 315, L269
Ott, T. 2004, Ph.D. Thesis
Reid, M. J., Menten, K. M., Genzel, R., et al. 2003, ApJ, 587, 208
Schödel, R., Ott, T., Genzel, R., et al. 2002, Nature, 419, 694
Shen, Z.-Q., Lo, K. Y., Liang, M.-C., Ho, P. T. P., & Zhao, J.-H. 2005, Nature, 438, 62
Stolovy, S. R., Hayward, T. L., & Herter, T. 1996, ApJ, 470, L45
Telesco, C. M., Davidson, J. A., & Werner, M. W. 1996, ApJ, 456, 541
Yuan, F., Markoff, S., & Falcke, H. 2002, A&A, 383, 854
Yuan, F., Quataert, E., & Narayan, R. 2003, ApJ, 598, 301
Yuan, F., Quataert, E., & Narayan, R. 2004, ApJ, 606, 894